VOLUME 81 PAPER No. 791

PROCEEDINGS

AMERICAN SOCIETY OF CIVIL ENGINEERS

SEPTEMBER, 1955

FLOW GEOMETRY AT STRAIGHT DROP SPILLWAYS

by Walter Rand, A.M. ASCE

HYDRAULICS DIVISION

(Discussion open until January 1, 1956)

Headquarters of the Society
33 W. 39th St.
New York 18, N. Y.

PRICE $0.50 PER COPY

THIS PAPER

--represents an effort by the Society to deliver technical data direct from the author to the reader with the greatest possible speed. To this end, it has had none of the usual editing required in more formal publication procedures.

Readers are invited to submit discussion applying to current papers. For this paper the final date on which a discussion should reach the Manager of Technical Publications appears on the front cover.

Those who are planning papers or discussions for "Proceedings" will expedite Division and Committee action measurably by first studying "Publication Procedure for Technical Papers" (Proceedings Paper No. 290). For free copies of this Paper—describing style, content, and format—address the Manager, Technical Publications, ASCE.

This paper was published at 1745 S. State Street, Ann Arbor, Mich., by the American Society of Civil Engineers. Editorial and General Offices are at 33 West Thirty-ninth Street, New York 18, N. Y.

FLOW GEOMETRY AT STRAIGHT DROP SPILLWAYS

Walter Rand,[1] A. M. ASCE

SYNOPSIS

The flow pattern at a straight drop spillway can be described by a number of characteristic length terms: the drop length, that is the distance from the vertical drop wall to the toe of the non-submerged nappe, the depth of flow at the toe of the nappe, the length of the hydraulic jump if it begins at the toe of the nappe, the depth of flow downstream from this jump, and the depth of the under-nappe pool between the drop wall and the nappe.[2] All these values are represented in this paper as functions of the discharge, and of the height of the drop. The results are given by a collective plot of dimensionless terms. Two geometrical properties of the flow pattern are established, consisting in practically constant relationships between some of the terms. The determination of flow geometry is important for the design of straight drop stilling basins.

NOTATIONS

The letter symbols are defined where they first appear and are assembled in the Glossary. They conform essentially to American Standard Letter Symbols for Hydraulics, prepared by the American Standards Association (ASA-Z10.2-1942).

Purpose and Scope of This Investigation

An investigation whose purpose was to develop a method of design for straight drop stilling basins was conducted by the writer at the Technical University of Karlsruhe in Germany in 1943.[3] Only the first part of these studies, dealing with the geometrical pattern of the non-uniform flow over a straight smooth non-erodable bottom immediately downstream of the drop, will be discussed in this paper. The formation of a stilling basin, by using such flow obstructions as baffles, sills, or abrupt rises in the bottom of the channel, will be discussed only briefly in the present introduction, to show how the design of the stilling basin depends on the original unobstructed flow at the drop.

---

1. Asst. Prof. of Fluid Mechanics, New York University, New York, N. Y.

2. Discussion by Walter Rand of "Equation of the Free-Falling Nappe", by Fred W. Blaisdell, Proceedings, Separate No. 624, ASCE, Feb., 1955.
3. "Die Sturzbett ausbildung bei lotrechten Absturzen und bei Anwendung einer rechteckigen Endschwelle," thesis submitted to the Technical University of Karlsruhe in Germany in partial fulfilment of the requirements for the degree of Doctor of Engineering.

The flow is considered to be two-dimensional that practically corresponds to the flow near to the centerline of a wide channel. The flow geometry at the drop depends on the discharge per unit width q, on the height of the drop h, and on the depth of uniform flow in the channel, up- and downstream from the drop structure. The study was limited to the subcritical flow in the up- and downstream channel, and to an aerated nappe. The flow will occur in this case either with a non-submerged or with a submerged nappe, depending on the downstream depth of the flow, and consequently on the hydraulic characteristics of the channel: slope, roughness, and hydraulic radius. Both flow types are given in Fig. 1, including the limiting case between the two (Fig. 1B), together with all the important length terms under consideration.

In Fig. 1A, the flow with non-submerged nappe is shown. The subcritical upstream flow passes to supercritical near to the crest of overflow, and has a depth $d_o = 0.715\ d_c$ over the crest, where d_c is the critical depth.[4] The free-falling nappe, with practically atmospheric pressure over the under-nappe pool of the depth d_f between the drop wall and the nappe, reverses its curvature, and turns smoothly into supercritical flow on the apron, at the distance l_d from the drop wall, marks the initial point of flow in the downstream channel. The distance l_d will be called the drop length in this paper. The mean velocity at the distance l_d from the drop wall is parallel to the apron, the depth d_1 at this place is the smallest depth in the downstream channel, and the pressure in the flow is nearly hydrostatic. Evidently, the drop length l_d is larger than the distance l_p at which the centerline of a free-falling nappe would hit the apron if the under-nappe pool were nonexistent.

The depth of supercritical flow in the downstream channel, initially d_1, will increase in the flow direction due to the channel resistance, and reach the depth d_3 at a certain distance that is sufficient for the formation of a stationary hydraulic jump between the supercritical flow and the uniform, subcritical flow of the depth d, determined by the hydraulic characteristics of the channel.

In Fig. 1B the limiting case is shown. The hydraulic jump of the length L begins with the depth d_1 and ends with the channel depth d_2 that is greater than d in Fig. 1A. The nappe is still non-submerged. However, no supercritical flow with a free surface exists on the apron, and the end of the hydraulic jump is the closest to the drop wall, compared with the cases in Fig. 1A and C.

In Fig. 1C the depth d of the channel flow is greater than d_2 and the nappe is submerged. The depth of the under-nappe pool is increased, and the turbulent surface roller extends farther downstream and is less intense than the hydraulic jump in Fig. 1B.

If the channel is erodable, a stilling basin is needed to protect the channel against the erosion. The design will depend on the flow geometry, classified in Fig. 1. It would be necessary to extend the apron, in the case of flow type in Fig. 1A, to the end of the hydraulic jump. However, there will be three more economical design solutions, where the hydraulic jump is created and kept at the toe of the fall. These are: (1) an apron at the bed level and an end sill or baffles, (2) an apron at an elevation below the downstream bed level, and an end sill that reaches higher than the downstream bed level, and (3) an apron at an elevation below the downstream bed level, and an end sill that is on level with the downstream bed, forming a step in the bottom. The choice of type of design and its dimensions will depend, for a given discharge q, on the drop height h and on the downstream depth d.

---

4. "Discharge Characteristics of the Free Overfall", by Hunter Rouse, Civil Engineering, April, 1936, p. 257.

In the case of flow type in Fig. 1B, the idea to extend the apron, without an end sill, to the end of the hydraulic jump, could be considered. However, a shorter and more economical stilling basin with an end sill will be possible, and better from the standpoint of the erosion. An apron deeper than the bed level is ordinarily not necessary. The flow type in Fig. 1C, with a long surface roller, may need a longer apron than in the case of the type shown in Fig. 1B. However, the end sill, when needed, will be relatively lower than it should be for the flow types in Figs. 1A and 1B. It is hoped that this short review of the design possibilities will illustrate the assumption that the geometry of the undisturbed flow should be taken into consideration for a sound design of a straight drop stilling basin.

Fundamental Considerations

The flow type for the limiting case in Fig. 1B includes all the important elements needed, and is therefore the topic of this investigation. All the dependent variables that determine the geometry of the flow, l_d, L, d_f, d_1, and d_2, are dependent on the two independent variables, h and q, where the last can be represented by the critical depth d_c:

$$d_c = \sqrt[3]{\frac{q^2}{g}} \qquad (1)$$

Consequently, all the variables are dimensionally length terms, and the results show that the dimensionless ratios l_d/h, L/h, d_f/h, d_1/h and d_2/h can be represented as functions of d_c/h. If the last term is written as

$$\frac{d_c}{h} = \sqrt[3]{\frac{q^2}{gh^3}} \qquad (2)$$

then the dimensionless ratio q^2/gh^3 can be adopted as an independent variable, that in a simple form describes the given flow by the primary variables q and h. The acceleration of gravity g in this ratio shows that the dynamic similarity is dependent on gravitational forces, as it primarily is for unconfined flow, if the small effect of viscosity and surface tension is neglected. In fact, this ratio, named drop number in this paper:

$$\underset{\sim}{D} = q^2/gh^3 \qquad (3)$$

is a product of the second power of the Froude number $\underset{\sim}{F} = \frac{V_1}{\sqrt{gd_1}}$ and of the third power of the ratio d_1/h, where V_1 is the velocity at the toe of the nappe, equal to q/d_1.

The results of the investigation are represented as a dimensionless plot in Fig. 4, using the drop number $\underset{\sim}{D}$ as the independent variable. The corresponding equations are written with $\underset{\sim}{D}$ or d_c/h as independent variables.

Of all the characteristic values under study, the drop length l_d has not been investigated previously, so far as the writer knows. The other values have been investigated by various authors. The writer refers here to the valuable paper by Dr. Walter Moore[5] that gives, together with the discussions, a very good description of the hydraulics of a vertical drop. In the present paper, in using the drop number $\underset{\sim}{D}$, a short way is offered to compute the needed values of flow geometry. Some constant relationships between the different terms are revealed (Eqs. 14 and 15).

---

5. "Energy Loss at the Base of Free Overfall", by Walter L. Moore, Transactions, ASCE, Vol. 108 (1943), p. 1343.

Experimental Procedure and Data

A vertical drop model, with the height of drop h = 7.79 in., was constructed in a 19.70 in. wide, rectangular plate glass flume. A smooth concrete bottom extended horizontally up- and downstream from the drop. The vertical drop wall was provided with a ventilating opening that secured a very nearly atmospheric pressure under the nappe. This could be concluded of the fact that the measured depth values of the under-nappe pool were only about 2% higher than the theoretical values, computed in applying the momentum principle and assuming atmospheric pressure under the nappe (similar application of the momentum principle: Moore[5], Eq. 8).

The flow was stilled by passing it through the screens, and was then measured by a 19.70 in. long suppressed sharp-crested weir. The flow depth in the downstream channel was controlled by movable steel blades, placed vertically into the channel, 14 ft. from the drop. The surface elevation of the flow at various points was measured with a point gage that could be moved along the rails above the channel. There was another point gage, mounted upon a damping well outside of the flume, to have a second possibility for measuring the tailwater elevation. The well was connected to the downstream channel by a rubber tube and a piezometric opening at the center-line of the bottom plate of the flume. The minimum reading of the vernier was 0.00033 ft. (0.1 mm). The measurements of different length terms and surface elevations for a given case of flow were repeated 20 times and the average values of these were inserted in the table of results (Table 1). This eliminated the measurement errors, caused by a strongly fluctuating flow surface.

The Fig. 1B shows that the drop length l_d has to be known so that the hydraulic jump at the toe of the nappe could be located exactly and the corresponding tailwater depth d_2 measured. However, l_d is unknown, and it cannot be measured very exactly directly from the flow pattern shown in Fig. 1A because of a very small change of flow depth along the apron at the toe of the nappe. Even if it could be done, it would be very difficult to arrange that the extremely turbulent beginning of the jump would lie exactly at the distance l_d from the drop wall. This is why the following procedure was adopted. For each discharge q, the distance l_j of the beginning of the hydraulic jump from the drop wall was measured as a variable, depending on the variable depth d in the downstream channel, that ranged from $d < d_2$ to $d > d_2$, covering all the flow types given in Fig. 1. The results for q = 124 cu. in. per sec. are given in Fig. 2.

The right part of the curve is convex and represents the flow type in Fig. 1A. The left part of the curve is concave and represents the flow type in Fig. 1C, where the changing tailwater depth causes only small changes in the distance l_j as the hydraulic jump starts to submerge the nappe. The point A, at which the curve is reversing its curvature indicates the beginning of the influence of the nappe on the tailwater depth by increasing depth of flow at the toe of the nappe in the direction of the drop wall, and by the non-hydrostatic pressure distribution in the flow in this region. As the beginning of the hydraulic jump moves to the left of point A, the end of the jump ceases to approach the drop wall and starts to move to the right again. The hydraulic jump changes into a long surface roller, shown in Fig. 1C. Consequently, the point A represents the initial point of flow in the downstream channel, and the distance of point A from the drop wall will be the drop length l_d. It can be determined relatively exactly from the drawing, together with the corresponding tailwater depth d_2.

TABLE 1

h inches	q in.^{3}/sec.	d_c/h	D	d_1/h	d_2/h	l_d/h	d_f/h
7.79		0.0464	0.0001				
	7.75		0.00033			0.455	
		0.1000	0.0010				
	15.50		0.00132	0.0339	0.290	0.734	
	31.0		0.0053	0.0531	0.416	1.012	0.33
		0.215	0.0100				
	46.5		0.0119	0.0760	0.510	1.318	
	62.0		0.0211	0.1002	0.595	1.42	0.46
	77.5		0.0330	0.122	0.671	1.72	
	93.0		0.0476	0.144	0.739	1.82	0.55
	108.5		0.0647	0.165	0.798	1.92	
	124.0		0.0846	0.190	0.856	2.13	0.61
		0.464	0.1000				
		1.000	1.0000				
Recalculated from Moore's data:							
18		0.0685	0.000322	0.0186	0.185		0.15
		0.085	0.00062	0.0247	0.22		0.18
	105	0.170	0.0049	0.056	0.39	1.05	0.31
	191	0.254	0.0162	0.095	0.56	1.44	0.42
		0.333	0.037	0.129	0.70		0.50
6		0.522	0.142	0.226	0.99		0.69
		1.000	1.000	0.532	1.68		1.00
Recalculated from the data of Bakhmeteff and Feodoroff:							
10.45	242	0.51	0.132			2.24	

The initial flow depth d_1 could be measured fairly well by repeated point gage measurements. The depth of the under-nappe pool d_f was measured from outside of the glass-walled flume as an average value of the distance between the bottom and the slightly sloped surface. A precision of $\pm$ 0.005 ft. was considered sufficient.

The experimental results, shown in Table 1, were supplemented for the sake of completeness by the corresponding values, recalculated from the data of Dr. Moore[5]. The results of both investigators are in good agreement and cover together a wide range of the drop number $\underset{\sim}{D}$. It seems that the difference in the channel width (Moore: 11 in. ; Rand: 19.7 in.) did not appreciably influence the results and that the flow in both cases was practically two-dimensional.

The drop length l_d was not measured by Dr. Moore. However, Fig. 6 and 10 in his paper show two flow profiles with the pressure variation along the bottom indicated. If l_d is taken as the distance between the drop wall and the point at which the hydrostatic pressure on the bottom begins, then l_d can be determined from the drawing. These values, and also one, determined from the surface profile for areated nappe in Fig. 20, in the discussion of Moore's paper by Professors Bakhmeteff and Feodoroff, agree closely with the results of the writer.

Discussion of the Results

All the data are plotted on log-log paper as a function of the drop number $\underset{\sim}{D}$ and they result in the well-defined relationships shown in Fig. 4. To represent all the characteristic values that determine the drop flow, the length of the hydraulic jump, that was not measured, has been inserted as $L = 6 (d_2 - d_1)$, averaging the measurements of Bakhmeteff, Matzke, and Moore[5].

The entire pattern of drop flow is represented by a simple graph in dimensionless form that corresponds to the model law in case the gravitational forces are predominant. The lower limit of the graph, $\underset{\sim}{D} = 0.0001$, corresponds to $d_c/h = 0.0464$, that represents a very high drop or a very low discharge. Still smaller values of $\underset{\sim}{D}$ are outside of the range of ordinary drop structures. The experiments were limited to about $\underset{\sim}{D} = 0.0003$, to avoid the excessive effect of the viscosity and surface tension on the model flow. The higher limit of the graph is given by $\underset{\sim}{D} = 1$ that corresponds to $d_c/h = 1$. This is the highest value for $\underset{\sim}{D}$ for free-falling nappe because, at this value, the depth of the under-nappe pool reaches the height of the drop h, and $d_f/h = 1$. A drop structure at $\underset{\sim}{D} = 1$ is more like a bottom sill, and corresponds to a very low drop height or to a very large discharge, both out of the ordinary range. As can be seen, the complete data given in Table 1 covers fairly well the entire range of $\underset{\sim}{D}$ values that correspond to the ordinary drop structures.

The effect of the loss of energy at the drop on the flow can be made apparent by computing the values d_1 and d_2 theoretically as d_{o1} and d_{o2}, without taking the losses into consideration, and plotting these values as shown in Fig. 4. The Bernoulli equation, written for the total head over the crest of the fall and at the toe of the nappe:

$$h + 1.5\, d_c = d_{o1} + \frac{q^2}{2g d_{o1}^2} \qquad (4)$$

5. "Energy Loss at the Base of Free Overfall", by Walter L. Moore, Transactions, ASCE, Vol. 108 (1943), p. 1343.

can be solved for d_{o1}, and do_{o2} can then be computed by the momentum equation for the hydraulic jump. The slightly curved plots of d_{o1}/h and d_{o2}/h in Fig. 4 show that due to the loss of energy, $d_{o1}/h < d_1/h$, and $d_{o2}/h > d_2/h$. The graphs for d_1/h and d_2/h are close to a straight line and can be approximated by the equations:

$$d_1/h = 0.54\,D^{0.425} \quad \text{or} \quad d_1/h = 0.54\,(d_c/h)^{1.275}, \tag{5}$$

and

$$d_2/h = 1.66\,D^{0.27} \quad \text{or} \quad d_2/h = 1.66\,(d_c/h)^{0.81} \tag{6}$$

From Eqs. 5 and 6 the height of the hydraulic jump at the base of the overfall can be expressed as

$$d_2/d_1 = 3.07/D^{0.155} \quad \text{or} \quad d_2/d_1 = 3.07/\,(d_c/h)^{0.465} \tag{7}$$

This is a close approximation, and corresponds well to the equation of the hydraulic jump:[6]

$$d_2/d_1 = \frac{1}{2}(\sqrt{1 + 8F^2} - 1) \tag{8}$$

where

$$F = \frac{V_1}{\sqrt{g d_1}} \quad .$$

The Froude number F can be expressed by the drop number D as follows (see page 3):

$$D = \frac{q^2}{g\ h^3} = \frac{V_1^{\,2} d_1^{\,2}}{g\ h^3} = F^2 \left(\frac{d_1}{h}\right)^3 , \tag{9}$$

or by inserting d_1/h from Eq. 5,

$$D = \frac{833}{F^{7.27}} \quad \text{or} \quad F = \frac{2.53}{D^{0.138}} \tag{10}$$

For the range of the investigated drop numbers the comparative values are:

D	F	d_2/d_1 (Eq. 7)	d_2/d_1 (Eq. 8)
0.0001	9.02	12.80	12.25
0.001	6.55	8.95	8.75
0.01	4.78	6.26	6.26
0.1	3.47	4.39	4.40
1	2.53	3.07	2.11

The measured values of the drop length ratio l_d/h, that form a fairly straight line in Fig. 4, are certainly larger than the corresponding values l_p/h, where the distance l_p is determined by the fall parabola (Fig. 1A). An approximate comparison can be made. If the horizontal velocity on the crest is taken as

$$v = \frac{q}{0.715\ d_c} \quad ,$$

and the small vertical velocity component is neglected, then from the motion equations

$$\frac{1}{2} g t^2 = h + \frac{0.715}{2}\,d_c \quad \text{and} \quad \frac{q\ t}{0.715\ d_c} = l_p ,$$

6. "Engineering Hydraulics," edited by Hunter Rouse, John Wiley and Sons, Inc., New York, 1950, p. 72.

where t is the fall time, it results that

$$\underline{l}_p/h = 1.98\sqrt{\frac{d_c}{h}\left(1 + 0.357\frac{d_c}{h}\right)} \quad , \tag{11}$$

or

$$\underline{l}_p/h = 1.98\sqrt{\underset{\sim}{D}^{1/3} + 0.357\,\underset{\sim}{D}^{2/3}} \quad , \tag{12}$$

shown in Fig. 4

The difference between $\underline{l}_d/h$ and $\underline{l}_p/h$, that would be even more pronounced if the vertical velocity component on the crest were taken into consideration, increases with increasing D and reaches the maximum ratio $\underline{l}_d/\underline{l}_p = 1.87$ at $D = 1$. For D 0.001 the difference of the two ratios is negligible. The computation of $\underline{l}_p/h$ is not sufficiently exact to determine the difference between $\underline{l}_d$ and $\underline{l}_p$ for drop values less than 0.002. The determination of $\underline{l}_d$ is important for the design of the stilling basin, and the introduction of $\underline{l}_p$ for $\underline{l}_d$ may lead to an unsatisfactory design, especially in the case of relatively low drop structures.

The experimental values of $\underline{l}_d/h$ closely follow the equation

$$\underline{l}_d/h = 4.30\,\underset{\sim}{D}^{0.27} \tag{13}$$

A constant relationship between $\underline{l}_d$ and d_2 will be established by dividing Eq. 13 by Eq. 6:

$$\underline{l}_d/d_2 = 2.60 \tag{14}$$

Another constant relationship, resulting from the experiments, is the practical exactness of the property of the nappe, that the three points, A- on the apron at the distance $\underline{l}_d$, B- on the axis of the nappe at the height d_f from the bottom, and C- on the axis of the nappe at the crest of the fall, lie on a straight line, shown in Fig. 3. Then

$$\frac{h + \frac{d_o}{2}}{\underline{l}_d} = \frac{d_f}{\underline{l}_d - \underline{l}_{pB}} \tag{15}$$

where $d_o/2 = 0.357\,d_c$. The distance $\underline{l}_{pB}$ of the axis of nappe from the drop wall at the elevation of d_f can be computed by Eq. 11 for the drop height $h-d_f$:

$$\underline{l}_{pB} = 1.98\,(h - d_f)\sqrt{\frac{d_c}{h - d_f}\left(1 + 0.357\,\frac{d_c}{h - d_f}\right)}$$

or

$$\underline{l}_{pB} = 1.98\sqrt{d_c\,(h + 0.357\,d_c - d_f)} \tag{16}$$

From Eqs. 15 and 16, the ratio $\underline{l}_d/h$ can be given as

$$\frac{\underline{l}_d}{h} = \frac{1.98\left(1 + 0.357\frac{d_c}{h}\right)\sqrt{\frac{d_c}{h}}}{\sqrt{1 + 0.357\,\frac{d_c}{h} - \frac{d_f}{h}}} \tag{17}$$

The line, that corresponds to Eq. 17 in Fig. 4, closely follows the experimental results when computed from the measured values of d_f. The geometrical relationships, given by Eqs. 14 and 15, help one to trace the flow surface at a drop structure with a minimum of computation.

The surface of the under-nappe pool is slightly sloped in the direction of the nappe, because the pool is rotating under the action of the overflow. The experimental values of d_f/h correspond to the mean depth. They form the flatly curved line in Fig. 4 that can be approximated by the straight line equation in the logarithmic plot

$$d_f/h = \underset{\sim}{D}^{0.22} \tag{18}$$

The length ratio L/h of the hydraulic jump is given by a slightly curved line in Fig. 4. It corresponds to the equation

$$L/h = 6\ (d_2/h - d_1/h) \tag{19}$$

as mentioned in the first paragraph of this chapter.

CONCLUSIONS

The flow geometry at a straight drop spillway can be represented by a dimensionless plot (Fig. 4), where all the charateristic length terms, d_f, d_1, d_2, l_d, and L (Fig. 1B) in the form of dimensionless ratios d_f/h, d_1/h, d_2/h, l_d/h, and L/h, are given as functions of the drop number $\underset{\sim}{D}$, that in the form of Eq. 3 includes the independent variables h, q, and g. It is important to note that the energy loss at the drop is included in the plot, and no additional computations are necessary to take it into consideration.

The geometrical ratios can be expressed by simple exponential equations of $\underset{\sim}{D}$, based on experiments, that can be used instead of the graph. The constant geometrical ratios, $l_d/d_2 = 2.60$ and Eq. 15 further simplify the tracing of the flow geometry.

The flow type on the drop (Fig. 1) determines the design of a stilling basin for the structure. For a given drop height h, and discharge q per unit width of the fall crest, the depth d_2 in the downstream channel (Fig. 1B) can be computed. By comparing the actual depth d with d_2, the flow type (A, B, or C in Fig. 1) can be determined. The various design possibilities for a stilling basin, according to the existing flow type, are briefly discussed in the first chapter. The author intends to give a detailed study of the design problems in a separate paper.

ACKNOWLEDGMENTS

The writer is indebted to the Technical University of Tallinn, Estonia, for the scholarship that made it possible for him to undertake the graduate study at Karlsruhe, and to Professor Dr.—Ing. Heinrich Wittmann and Professor Dr.—Ing. Paul Boss, who suggested the study of the interesting problem of stilling basins and permitted me to conduct experimental work in the "Theodore Rehbock Flussbaulaboratorium" at the Technical University of Karlsruhe.

GLOSSARY

D = drop number = $\frac{q^2}{g\,h^3}$

d = the depth of uniform subcritical flow in the downstream channel.

d_c = the critical depth = $\sqrt[3]{\frac{q^2}{g}}$

d_f = the depth of the under-nappe pool between the drop wall and the nappe.

d_f^1 = the depth d_f in the case of submerged nappe.

d_o = the depth of flow at the crest of the fall = 0.715 d_c

d_1 = the depth at the toe of the nappe, at the distance $\underline{1}_d$ from the drop wall.

d_2 = the depth in the downstream channel in the case the hydraulic jump starts at the toe of the nappe, at the distance $\underline{1}_d$ from the drop wall.

d_3 = the depth of supercritical flow in the downstream channel at the beginning of the hydraulic jump.

d_{o1} = d_{o2} } theoretical values of d_1 and d_2, computed without taking into consideration the loss of energy at the drop.

$\underset{\approx}{F}$ = Froude number = $\frac{V_1}{\sqrt{gd_1}}$

g = acceleration of gravity.

h = height of the drop.

L = the length of the hydraulic jump that starts at the toe of the nappe, at the distance 1_d from the drop wall.

$\underline{1}$ = the distance between the toe of the nappe and the downstream end of the hydraulic jump.

$\underline{1}_d$ = the drop length, that is, the distance from the drop wall to the position of the depth d_1.

$\underline{1}_j$ = the distance between the drop wall and the beginning of hydraulic jump.

$\underline{1}_p$ = the distance of the point from the drop wall, at which the centerline of the free-falling nappe would hit the apron, if the under-nappe pool were nonexistent.

$\underline{1}_{pB}$ = the distance of the axis of the nappe from the drop wall at the elevation of d_f.

q = the discharge per unit width of the crest of overfall.

V_c = critical velocity = $\sqrt{gd_c}$.

V_1 = the velocity at the toe of the nappe = q/d_1.

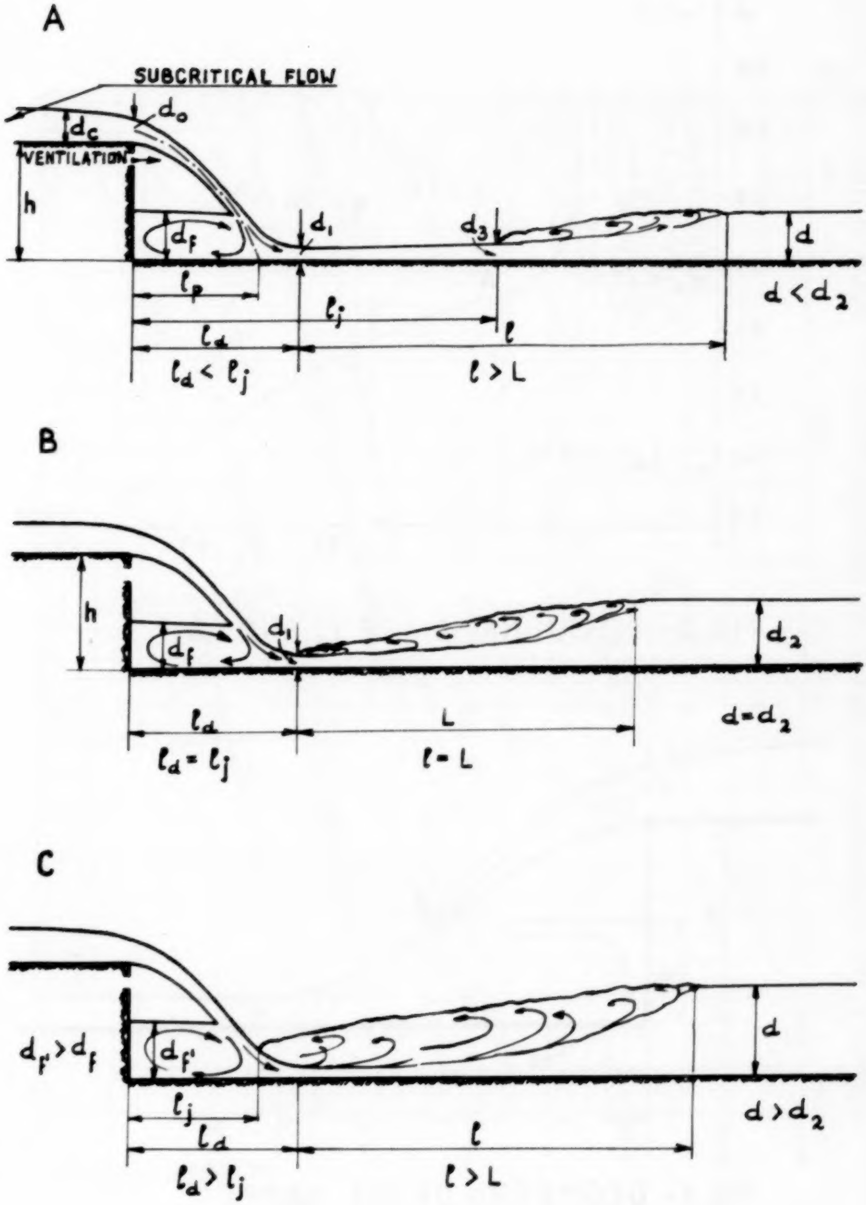

FIG. 1- FLOW TYPES AT STRAIGHT DROP SPILLWAY

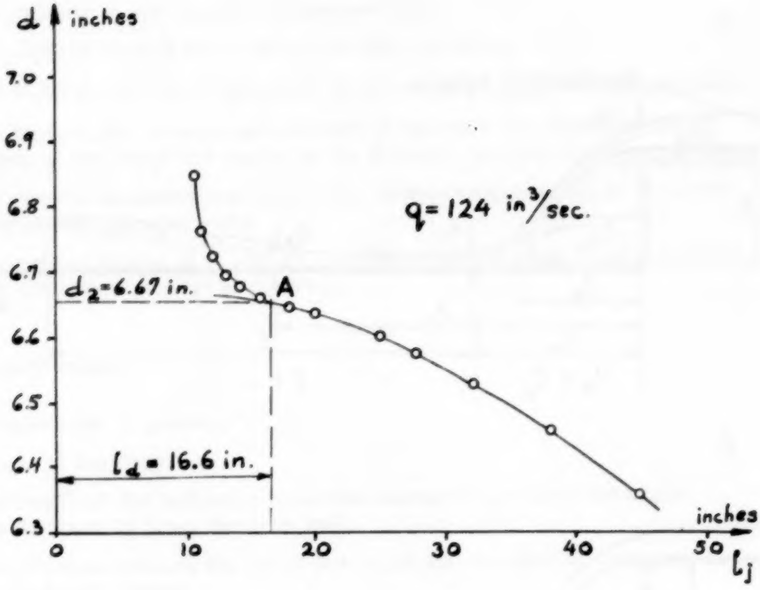

FIG.2 - DETERMINATION OF l_d AND d_2

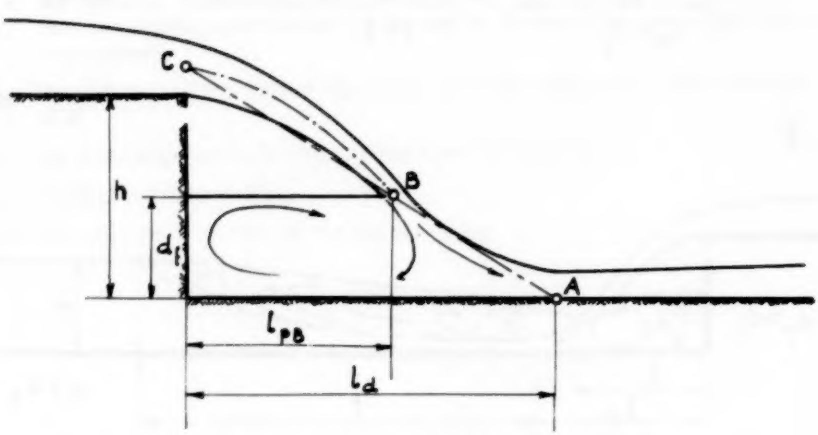

FIG.3 - GEOMETRY OF THE NAPPE

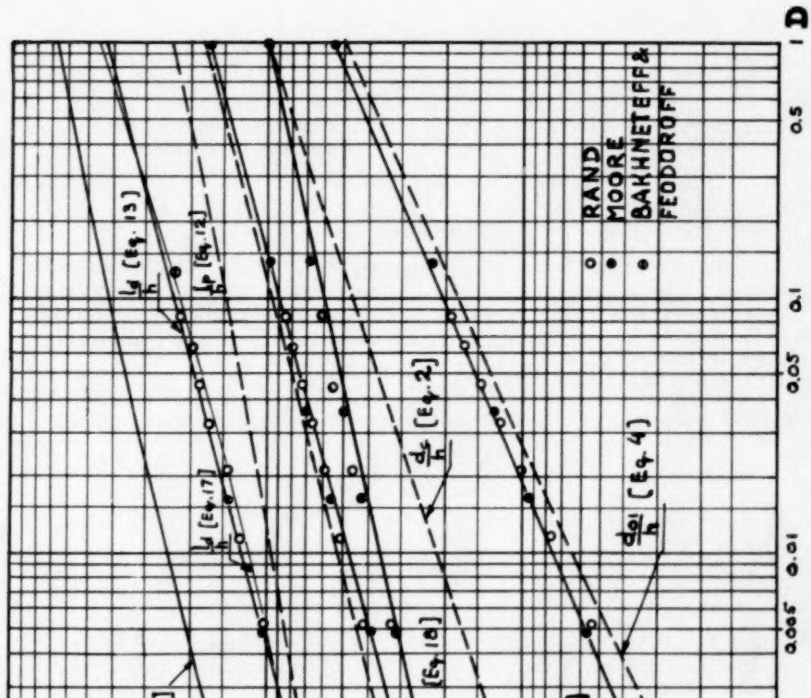

FIG. 4 - FLOW GEOMETRY AT STRAIGHT DROP SPILLWAY vs. DROP NUMBER D